



## Epitaxial growth of non-c-oriented SrBi<sub>2</sub>Nb<sub>2</sub>O<sub>9</sub> on (111) SrTiO<sub>3</sub>

J. Lettieri, M. A. Zurbuchen, Y. Jia, D. G. Schlom, S. K. Streiffer, and M. E. Hawley

Citation: *Applied Physics Letters* **76**, 2937 (2000); doi: 10.1063/1.126522

View online: <http://dx.doi.org/10.1063/1.126522>

View Table of Contents: <http://scitation.aip.org/content/aip/journal/apl/76/20?ver=pdfcov>

Published by the [AIP Publishing](#)

---

### Articles you may be interested in

Epitaxial growth of multiferroic BiFeO<sub>3</sub> thin films with (101) and (111) orientations on (100) Si substrates  
*Appl. Phys. Lett.* **102**, 242906 (2013); 10.1063/1.4811484

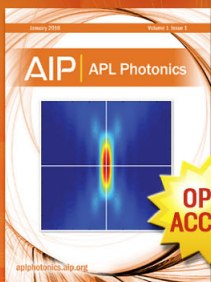
Growth and characterization of non-c-oriented epitaxial ferroelectric SrBi<sub>2</sub>Ta<sub>2</sub>O<sub>9</sub> films on buffered Si(100)  
*Appl. Phys. Lett.* **77**, 3260 (2000); 10.1063/1.1324982

Epitaxial growth of SrBi<sub>2</sub>Nb<sub>2</sub>O<sub>9</sub> on (110) SrTiO<sub>3</sub> and the establishment of a lower bound on the spontaneous polarization of SrBi<sub>2</sub>Nb<sub>2</sub>O<sub>9</sub>  
*Appl. Phys. Lett.* **77**, 3090 (2000); 10.1063/1.1322055

Epitaxial Pb(Mg<sub>1/3</sub>Nb<sub>2/3</sub>)O<sub>3</sub> thin films synthesized by metal-organic chemical vapor deposition  
*Appl. Phys. Lett.* **76**, 3106 (2000); 10.1063/1.126538

Structural and electrical characterization of epitaxial, large area ferroelectric films of Ba<sub>2</sub>Bi<sub>4</sub>Ti<sub>5</sub>O<sub>18</sub> grown by pulsed excimer laser ablation  
*J. Appl. Phys.* **87**, 2825 (2000); 10.1063/1.372263

---



Launching in 2016!  
The future of applied photonics research is here

AIP | APL  
Photonics

## Epitaxial growth of non-*c*-oriented SrBi<sub>2</sub>Nb<sub>2</sub>O<sub>9</sub> on (111) SrTiO<sub>3</sub>

J. Lettieri, M. A. Zurbuchen, Y. Jia,<sup>a)</sup> and D. G. Schlom<sup>b)</sup>

*Department of Materials Science and Engineering, The Pennsylvania State University, University Park, Pennsylvania 16803-6602*

S. K. Streiffer

*Materials Science Division, Argonne National Laboratory, Argonne, Illinois 60439*

M. E. Hawley

*Materials Science and Technology Division, Los Alamos National Laboratory, Los Alamos, New Mexico 87545*

(Received 23 November 1999; accepted for publication 22 March 2000)

Epitaxial SrBi<sub>2</sub>Nb<sub>2</sub>O<sub>9</sub> thin films have been grown with a (103) orientation on (111) SrTiO<sub>3</sub> substrates by pulsed-laser deposition. Four-circle x-ray diffraction and transmission electron microscopy reveal nearly phase-pure epitaxial films. Epitaxial (111) SrRuO<sub>3</sub> electrodes enabled the electrical properties of these (103)-oriented SrBi<sub>2</sub>Nb<sub>2</sub>O<sub>9</sub> films to be measured. The low-field relative permittivity was 185, the remanent polarization was 15.7 μC/cm<sup>2</sup>, and the dielectric loss was 2.5% for a 0.5-μm-thick film. © 2000 American Institute of Physics. [S0003-6951(00)01720-4]

Growth of single crystals often represents the first key step in the probing of a highly anisotropic material's fundamental properties. Bulk synthesis methods, although the most direct path to this end, can often be complicated by processing limitations, including uncharted phase equilibria and incongruent phase transformations. In many of these cases, epitaxial thin-film growth offers a viable alternative. Notwithstanding, growth of epitaxial thin films has its own complications. For example, substrate choice is critical for successful growth; substrates must be chemically compatible and closely lattice matched to the film. Additionally, the study of ferroelectrics and dielectrics generally entails the growth of an underlying epitaxial electrode. For many of the ferroelectrics that have received considerable attention recently, such as those of the Aurivillius<sup>1</sup> family of compounds (e.g., SrBi<sub>2</sub>Ta<sub>2</sub>O<sub>9</sub> and SrBi<sub>2</sub>Nb<sub>2</sub>O<sub>9</sub>), lattice match and chemical compatibility with a number of substrates and electrode candidates have already begun to be addressed. Given the perovskite-related structures of these compounds, growth of *c*-axis films on (001) perovskite substrates [i.e., SrTiO<sub>3</sub>, LaAlO<sub>3</sub>, NdGaO<sub>3</sub>, and LaAlO<sub>3</sub>-Sr<sub>2</sub>AlTaO<sub>6</sub> (LSAT)],<sup>2-5</sup> and perovskite electrodes (La,Sr)<sub>2</sub>CuO<sub>4</sub>, (La,Sr)CoO<sub>3</sub>, SrRuO<sub>3</sub>, and Sr<sub>2</sub>RuO<sub>4</sub>,<sup>6,7</sup> is a logical and demonstrated route. However, for ferroelectrics such as SrBi<sub>2</sub>Nb<sub>2</sub>O<sub>9</sub> that exhibit mirror inversion symmetry perpendicular to the *c* axis (and, consequently, a spontaneous polarization vector which lies entirely in the *a*-*b* plane and specifically along only the *a* axis),<sup>8</sup> probing of a film with a (001) orientation reveals little about the fundamental properties (spontaneous polarization and fatigue resistance) of the material. The challenge in studying the anisotropy of these compounds thus lies in growing films with orientations in which some component of the *a* axis is nonparallel to the substrate surface.

Although variation of process variables has been shown to control orientation in other perovskite-based systems such as YBa<sub>2</sub>Cu<sub>3</sub>O<sub>7</sub>,<sup>9,10</sup> analogous results have not been achieved

with the Aurivillius compounds. Indeed, previous research has revealed a relatively small parameter space for the phase-pure, epitaxial growth of these materials, with even minor deviation leading to the formation of impurity phases and intergrowths.<sup>2,11</sup> Other strategies have been employed, including the use of more esoteric and nonperovskite substrates in attempts to stabilize (110)- and (100)-oriented growth.<sup>2,12</sup> Although successful, this approach presents its own difficulties, including reproducibility, cost, and problems associated with the growth of an electrode/ferroelectric epitaxial heterostructure. Here, we present a third strategy: growth of SrBi<sub>2</sub>Nb<sub>2</sub>O<sub>9</sub> (Ref. 13) on non-{001}-oriented perovskite substrates.

Similar schemes have been used for the growth of oxide superconductors with perovskite-related structures.<sup>9,14-16</sup> Each of these prior studies discusses the growth of perovskite-based superconductors on a (110) SrTiO<sub>3</sub> surface, and indicates a dominant growth direction of (001) film || (001) SrTiO<sub>3</sub> substrate. Indeed, our previous work and related studies have shown this also to be true with SrBi<sub>2</sub>Nb<sub>2</sub>O<sub>9</sub> on (110) SrTiO<sub>3</sub>.<sup>17,18</sup> In an attempt to further increase the projection of the spontaneous polarization vector perpendicular to the substrate (i.e., increase the angle between the film *c* axis and the substrate normal), we explored the growth of SrBi<sub>2</sub>Nb<sub>2</sub>O<sub>9</sub> on (111) SrTiO<sub>3</sub>.<sup>19,20</sup> In this letter, we present the application of this approach for the probing of the ferroelectric properties of SrBi<sub>2</sub>Nb<sub>2</sub>O<sub>9</sub>.

SrBi<sub>2</sub>Nb<sub>2</sub>O<sub>9</sub> films were grown *in situ* by pulsed-laser deposition (PLD) using a KrF excimer laser (248 nm, Lambda Physik EMG103MSC) in an on-axis geometry. Films were grown in a 110 mTorr O<sub>3</sub>/O<sub>2</sub> mix (~8% O<sub>3</sub>) at a temperature of 877 °C provided by a radiative substrate heater.<sup>21</sup> A laser pulse energy of 150 mJ, fluence of 2-3 J/cm<sup>2</sup>, and a 4 Hz pulse rate were used to grow films ~0.5 μm thick. A single target with a Sr:Bi:Nb atom ratio of 1:2.3:2 was used as the source material. After growth, the films were quenched in 1 atm of oxygen. Details concerning target fabrication and optimization of the growth of these bismuth-based compounds are found elsewhere.<sup>11</sup>

<sup>a)</sup>On leave from Qingdao University, People's Republic of China

<sup>b)</sup>Electronic mail: schlom@ems.psu.edu

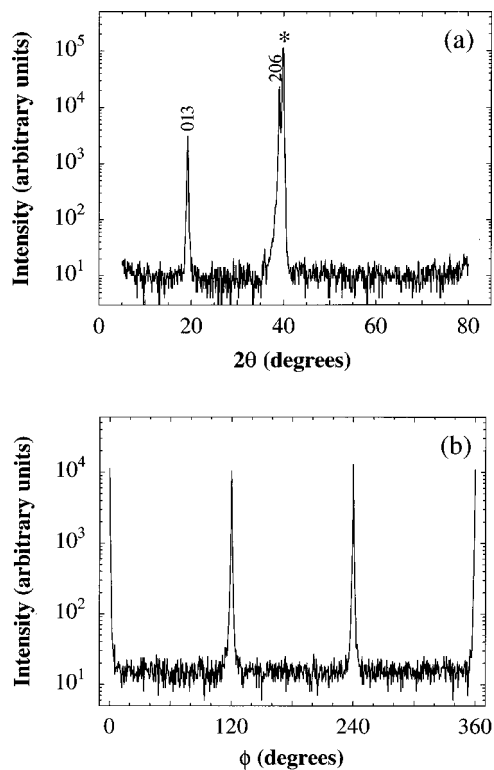


FIG. 1. (a)  $\theta$ - $2\theta$  x-ray diffraction plot of  $\text{SrBi}_2\text{Nb}_2\text{O}_9$  grown on a (111)  $\text{SrTiO}_3$  substrate indicating that the  $\text{SrBi}_2\text{Nb}_2\text{O}_9$  film is (103) oriented. Substrate peaks are labeled as (\*). (b)  $\phi$  scan of the 002  $\text{SrBi}_2\text{Nb}_2\text{O}_9$  reflection at  $\chi=33.4^\circ$ , indicating that the film is epitaxial.  $\chi=90^\circ$  is defined as perpendicular to the plane of the substrate.  $\phi=0^\circ$  is aligned to be parallel to the  $[1\ 1\ 2]$  in-plane direction of  $\text{SrTiO}_3$ . From these scans the lattice parameters of the  $\text{SrBi}_2\text{Nb}_2\text{O}_9$  film are  $a \approx b = 5.51 \pm 0.05 \text{ \AA}$  and  $c = 25.1 \pm 0.2 \text{ \AA}$ .

Heterostructures consisting of an underlying (111)  $\text{SrRuO}_3$  epitaxial electrode and an epitaxial (103)  $\text{SrBi}_2\text{Nb}_2\text{O}_9$  overlayer were prepared to investigate the electrical properties of the  $\text{SrBi}_2\text{Nb}_2\text{O}_9$  films.  $\text{SrRuO}_3$ , nearly lattice matched with  $\text{SrTiO}_3$  (Ref. 22) and chemically compatible with both the ferroelectric and substrate, proves to be an excellent choice.<sup>23</sup>  $\text{SrRuO}_3$  electrodes were grown with a stoichiometric target (99.9% purity, Target Materials, Inc.) at  $600^\circ\text{C}$  and 100 mTorr  $\text{O}_2$  with all other growth parameters as described previously for the growth of  $\text{SrBi}_2\text{Nb}_2\text{O}_9$ . Top platinum electrodes (250  $\mu\text{m}$  diam) were deposited through a shadow mask by  $e$ -beam evaporation at  $350^\circ\text{C}$ .

To characterize the films for phase purity and epitaxial orientation, a four-circle x-ray diffractometer with  $\text{Cu } K\alpha$  radiation and a graphite monochromator was used. Additional structural analysis was completed by transmission electron microscopy (TEM).<sup>27</sup>

Figure 1(a) shows a  $\theta$ - $2\theta$  x-ray diffraction scan of a  $\text{SrBi}_2\text{Nb}_2\text{O}_9$  film grown on (111)  $\text{SrTiO}_3$ . The scan reveals a nearly phase-pure (103)-oriented film. As with growth on (110)  $\text{SrTiO}_3$ ,<sup>17</sup> this growth can alternatively be described as (001)  $\text{SrBi}_2\text{Nb}_2\text{O}_9 \parallel$  (001)  $\text{SrTiO}_3$ , with (in this case) the  $c$  axis at  $\sim 57^\circ$  to the substrate normal. The full width at half maximum (FWHM) of the 206 reflection of  $\text{SrBi}_2\text{Nb}_2\text{O}_9$  is  $0.23^\circ$  and  $0.39^\circ$  in  $2\theta$  and  $\omega$ , respectively. Figure 1(b) shows a  $\phi$  scan of the 002  $\text{SrBi}_2\text{Nb}_2\text{O}_9$  reflection for the same film with a FWHM in  $\phi$  of  $\sim 1.1^\circ$ . The 002 reflection (rather than the more intense 0010 reflection or commonly used 115 reflection) was used because its relatively high  $d$  value

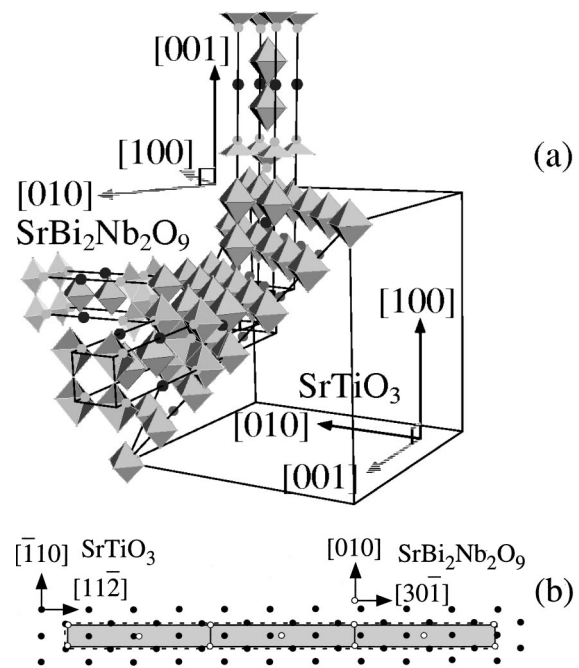


FIG. 2. (a) Schematic of the orientation relationship between the (103)  $\text{SrBi}_2\text{Nb}_2\text{O}_9$  film (all three epitaxial domain variants) and underlying (111)  $\text{SrTiO}_3$  substrate. The  $\text{SrBi}_2\text{Nb}_2\text{O}_9$  is drawn and its unit cell is outlined in its tetragonal state above its Curie temperature ( $\sim 430^\circ\text{C}$ , Ref. 19). Note that the growth temperature is well above the Curie temperature of  $\text{SrBi}_2\text{Nb}_2\text{O}_9$ , so the crystallography shown is relevant during nucleation and growth of the epitaxial film. The oxygen coordination polyhedra of the  $\text{TiO}_6$  octahedra in the topmost layer of the substrate and  $\text{NbO}_6$  octahedra and  $\text{Bi}_2\text{O}_2$  layers in the film are shown. The strontium atoms are depicted as dark dots in the film and topmost layer of the substrate. (b) Schematic showing surface meshes of the film and substrate for one of the three observed orientations. The substrate and film surface meshes are represented with black and white dots, respectively. The near-coincident site surface mesh cell is represented with a dashed line. The mesh mismatch at room temperature is 0.2% along the  $[\bar{1}10]$  substrate direction and 0.8% along the  $[11\bar{2}]$  substrate direction.

(12.55  $\text{\AA}$ ) (Ref. 13) allows it to be used for unambiguous phase and orientation determination. The  $\phi$  scan reveals a triple-domain film (ignoring the  $a$ - $b$  twinning in  $\text{SrBi}_2\text{Nb}_2\text{O}_9$ , which our x-ray measurements cannot discern), as expected for a film grown on a substrate with threefold symmetry.<sup>24</sup> Together, these x-ray scans indicate that the epitaxial orientation relationship is (103)  $\text{SrBi}_2\text{Nb}_2\text{O}_9 \parallel$  (111)  $\text{SrTiO}_3$  and (i)  $[010] \text{ SrBi}_2\text{Nb}_2\text{O}_9 \parallel [\bar{1}10] \text{ SrTiO}_3$ , (ii)  $[\bar{3}31] \text{ SrBi}_2\text{Nb}_2\text{O}_9 \parallel [\bar{1}10] \text{ SrTiO}_3$ , or (iii)  $[\bar{3}3\bar{1}] \text{ SrBi}_2\text{Nb}_2\text{O}_9 \parallel$

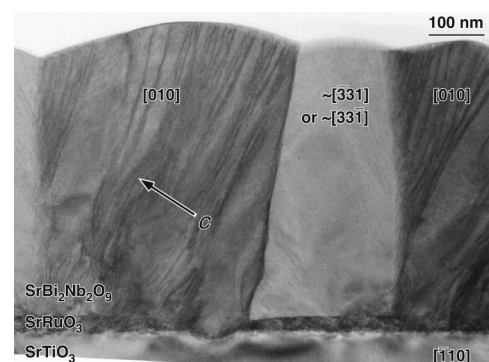


FIG. 3. Cross-sectional TEM image along the  $[\bar{1}10]$   $\text{SrTiO}_3$  zone axis of the same (103)  $\text{SrBi}_2\text{Nb}_2\text{O}_9 / (111) \text{ SrRuO}_3 / (111) \text{ SrTiO}_3$  film on which the hysteresis curve shown in Fig. 4 was measured. The zone axes of the epitaxial  $\text{SrBi}_2\text{Nb}_2\text{O}_9$  grains, of which there are three variants, are labeled. The direction of the  $c$  axis is indicated in one of the  $\text{SrBi}_2\text{Nb}_2\text{O}_9$  grains.

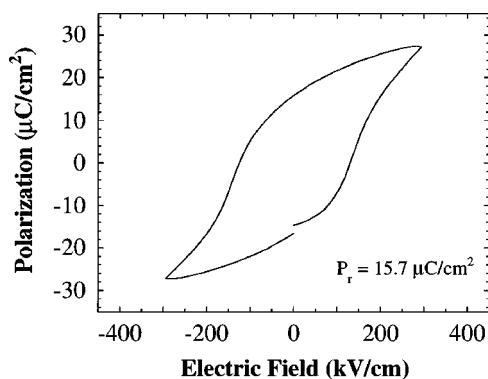


FIG. 4. Polarization–electric-field hysteresis curve for (103)  $\text{SrBi}_2\text{Nb}_2\text{O}_9$  on an epitaxial (111)  $\text{SrRuO}_3$  electrode. The remanent polarization is  $15.7 \mu\text{C}/\text{cm}^2$ . A cross-sectional TEM image of the same film on which this hysteresis curve was measured is shown in Fig. 3.

$[\bar{1}10]$   $\text{SrTiO}_3$  for the in-plane orientations (ignoring the  $a$ – $b$  twinning in  $\text{SrBi}_2\text{Nb}_2\text{O}_9$ ) of the three degenerate epitaxial orientations. These orientations are schematically shown in Fig. 2(a). This growth is not only a local continuation of the perovskite sublattice, but can also be considered in terms of the areal match of near-coincident site surface meshes of the (103)  $\text{SrBi}_2\text{Nb}_2\text{O}_9$  and the (111)  $\text{SrTiO}_3$  substrate. Consideration of these surface meshes with the observed epitaxial relationship results in a mismatch  $[(A_{\text{sub}} - A_{\text{film}})/A_{\text{film}}]$ , of 1.0% at room temperature for a substrate mesh with an area  $A_{\text{sub}} = 501.8 \text{ \AA}^2$  and a film mesh with area  $A_{\text{film}} = 496.7 \text{ \AA}^2$  [see Fig. 2(b)].

The epitaxial orientation of the  $\text{SrBi}_2\text{Nb}_2\text{O}_9$  films remained the same when they were grown on  $\text{SrRuO}_3$  epitaxial electrodes, i.e., (103)  $\text{SrBi}_2\text{Nb}_2\text{O}_9 \parallel (111) \text{SrRuO}_3 \parallel (111) \text{SrTiO}_3$  (x ray not shown).<sup>25</sup> A cross-sectional TEM image of such an epitaxial heterostructure is shown in Fig. 3. TEM analysis showed a lack of amorphous material (that would not be detected by x-ray diffraction analysis alone) and corroborated the epitaxial orientation relationships and phase purity deduced from the x-ray diffraction analysis.<sup>27</sup> Dark striations running roughly vertically in the  $[010]$  grains are out-of-phase boundaries (OPBs).<sup>26</sup>

Figure 4 shows the polarization–electric-field hysteresis of (103)  $\text{SrBi}_2\text{Nb}_2\text{O}_9$  measured on an RT6000. The remanent polarization ( $P_r$ ) was determined to be  $15.7 \mu\text{C}/\text{cm}^2$ . Low-field relative permittivity and dielectric loss ( $\tan \delta$ ) were 185 and 2.5%, respectively, for films measured on an HP 4192A at 10 kHz and a  $0.1 V_{\text{rms}}$  oscillation level.  $P_r$  values of  $12.5 \mu\text{C}/\text{cm}^2$  have previously been reported for randomly oriented  $\text{SrBi}_2\text{Nb}_2\text{O}_9$  thin films.<sup>28</sup> These results demonstrate the validity of our approach: to increase the usable polarization in thin-film heterostructures through orientation control. This is also a critical step to establishing and understanding the fundamental ferroelectric characteristics of this material.

The authors acknowledge the financial support of the U.S. Department of Energy through Grant No. DE-FG02-97ER45638 for the work performed at Penn State, Contract No. W-31-109-ENG-38 for the work performed at ANL, and use of the ANL Electron Microscopy Center. One of the authors (Y.J.) acknowledges the China Scholarship Council for financial support during his visit to Penn State.

- <sup>1</sup>B. Aurivillius, Ark. Kemi **1**, 463 (1950); **1**, 499 (1950); **2**, 519 (1951); **5**, 39 (1953); B. Aurivillius and P. H. Fang, Phys. Rev. **126**, 893 (1962).
- <sup>2</sup>J. Lettieri, Y. Jia, M. Urbanik, C. I. Weber, J.-P. Maria, D. G. Schlom, H. Li, R. Ramesh, R. Uecker, and P. Reiche, Appl. Phys. Lett. **73**, 2923 (1998).
- <sup>3</sup>J. Lettieri, M. A. Zurbuchen, G. W. Brown, Y. Jia, W. Tian, X. Q. Pan, M. E. Hawley, and D. G. Schlom, in *Multicomponent Oxide Films for Electronics*, edited by M. E. Hawley, D. H. A. Blank, C. B. Eom, D. G. Schlom, and S. K. Streiffer (Materials Research Society, Pittsburgh, PA, 1999), Vol. 574, pp. 31–36.
- <sup>4</sup>Q. D. Jiang, Z. J. Huang, P. Jin, C. L. Chen, A. Brazdeikis, Y. Y. Sun, H. H. Feng, A. Benneker, and C. W. Chu, Surf. Sci. Lett. **405**, L554 (1998).
- <sup>5</sup>J. H. Cho, S. H. Bang, J. H. Son, and Q. X. Jia, Appl. Phys. Lett. **72**, 665 (1998).
- <sup>6</sup>J. Lettieri, Y. Jia, M. Urbanik, C. I. Weber, J.-P. Maria, R. Uecker, P. Reiche, and D. G. Schlom, presented at the 10th International Symposium on Integrated Ferroelectrics, Monterey, CA, 1998 (unpublished).
- <sup>7</sup>S. J. Hyun, B. H. Park, S. D. Bu, J. H. Jung, and T. W. Noh, Appl. Phys. Lett. **73**, 2518 (1998).
- <sup>8</sup>R. E. Newnham, R. W. Wolfe, and J. F. Dorrian, Mater. Res. Bull. **6**, 1029 (1971).
- <sup>9</sup>T. Terashima, Y. Bando, K. Iijima, K. Yamamoto, and K. Hirata, Appl. Phys. Lett. **53**, 2232 (1988).
- <sup>10</sup>J. Fujita, T. Yoshitake, A. Kamijo, T. Satoh, and H. Igarashi, J. Appl. Phys. **64**, 1292 (1988).
- <sup>11</sup>J. Lettieri, Y. Jia, S. Fulk, D. G. Schlom, M. E. Hawley, and G. W. Brown, Thin Solid Films (submitted).
- <sup>12</sup>S. E. Moon, T. K. Song, S. B. Back, S.-I. Kwun, J.-G. Yoon, and J. S. Lee, Appl. Phys. Lett. **75**, 2827 (1999).
- <sup>13</sup> $\text{SrBi}_2\text{Nb}_2\text{O}_9$  is orthorhombic with space group  $A2_1am$  and lattice constants  $a = 5.5094 \text{ \AA}$ ,  $b = 5.5094 \text{ \AA}$ , and  $c = 25.098 \text{ \AA}$  at room temperature as determined by A. D. Rae, J. G. Thompson, R. L. Withers, and A. C. Willis, Acta Crystallogr., Sect. B: Struct. Sci. **B46**, 474 (1990).
- <sup>14</sup>J. Kwo, R. M. Fleming, H. L. Kao, D. J. Werder, and C. H. Chen, Appl. Phys. Lett. **60**, 1905 (1992).
- <sup>15</sup>C. B. Eom, A. F. Marshall, Y. Suzuki, R. Boyer, R. F. Pease, and T. H. Geballe, Nature (London) **353**, 544 (1991).
- <sup>16</sup>K. Kuroda, O. Wada, J. Tanimura, K. Kojima, T. Takami, M. Kataoka, T. Ogama, and K. Hamanaka, Jpn. J. Appl. Phys., Part 2 **30**, L582 (1991).
- <sup>17</sup>J. Lettieri, M. A. Zurbuchen, G. W. Brown, Y. Jia, W. Tian, X. Q. Pan, M. E. Hawley, and D. G. Schlom, presented at the Spring 1999 Materials Research Society Meeting, San Francisco, CA, 1999 (unpublished).
- <sup>18</sup>T. Nagahama, T. Manabe, I. Yamaguchi, T. Kumagai, T. Tsuchiya, and S. Mizuta, Thin Solid Films **353**, 52 (1999).
- <sup>19</sup>*Numerical Data and Functional Relationships in Science and Technology*, Landolt-Börnstein Series, edited by K.-H. Hellwege and A. M. Hellwege (Springer, Berlin, 1976), New Series, Group III, Vol. 7, Part e, pp. 134–135; (Springer, Berlin, 1977), Vol. 7, Part f, p. 743; (Springer, Berlin, 1981), Vol. 16, Part a, p. 233.
- <sup>20</sup> $\text{SrTiO}_3$  is cubic with space group  $Pm3m$  and lattice constant  $a = 3.905 \text{ \AA}$  (see Ref. 19) at room temperature.
- <sup>21</sup>J. C. Clark, J.-P. Maria, K. J. Hubbard, and D. G. Schlom, Rev. Sci. Instrum. **68**, 2538 (1997).
- <sup>22</sup> $\text{SrRuO}_3$  is orthorhombic with space group  $Pbnm$  and lattice constants  $a = 5.53 \text{ \AA}$ ,  $b = 5.57 \text{ \AA}$ , and  $c = 7.85 \text{ \AA}$  at room temperature (see Ref. 19). The lattice can be considered as a pseudocubic perovskite with  $a \approx 3.92 \text{ \AA}$  resulting in a  $-0.5\%$  lattice mismatch with  $\text{SrTiO}_3$  at room temperature. We use pseudocubic indexing throughout this manuscript for  $\text{SrRuO}_3$ .
- <sup>23</sup>C. B. Eom, R. J. Cava, R. M. Fleming, J. M. Phillips, R. B. van Dover, J. H. Marshall, J. W. P. Hsu, J. J. Krajewski, and W. F. Peck, Jr., Science **258**, 1766 (1992).
- <sup>24</sup>S.-W. Chan, J. Phys. Chem. Solids **55**, 1137 (1994).
- <sup>25</sup>The narrowest FWHMs observed were  $0.23^\circ$  in  $2\theta$  and  $0.62^\circ$  in  $\omega$  for the 206 peak of  $\text{SrBi}_2\text{Nb}_2\text{O}_9$  for films grown on (111)  $\text{SrRuO}_3$  electrodes on (111)  $\text{SrTiO}_3$ .
- <sup>26</sup>We observe OPBs in all of our epitaxial  $\text{SrBi}_2\text{Nb}_2\text{O}_9$  and  $\text{SrBi}_2\text{Ta}_2\text{O}_9$  films grown by PLD on (001), (110), and (111)  $\text{SrTiO}_3$  substrates, both with and without  $\text{SrRuO}_3$  electrodes, and also on (110)  $\text{NdGaO}_3$  substrates.
- <sup>27</sup>M. A. Zurbuchen, J. Lettieri, Y. Jia, and D. G. Schlom, J. Mater. Res. (submitted).
- <sup>28</sup>K. Watanabe, M. Tanaka, E. Sumitomo, K. Katori, H. Yagi, and J. F. Scott, Appl. Phys. Lett. **73**, 126 (1998).